



# Effect of Root Diameter on the Selection and Network Interactions of Root-Associated Bacterial Microbiomes in *Robinia pseudoacacia* L

Xiaoyu Zai<sup>1</sup> · Wen Luo<sup>1</sup> · Wenqing Bai<sup>1</sup> · Yuhua Li<sup>1</sup> · Xiao Xiao<sup>2</sup> · Xuee Gao<sup>1</sup> · Entao Wang<sup>3</sup> · Gehong Wei<sup>1</sup> · Weimin Chen<sup>1</sup>

Received: 16 August 2020 / Accepted: 29 December 2020 / Published online: 15 January 2021  
© The Author(s), under exclusive licence to Springer Science+Business Media, LLC part of Springer Nature 2021

## Abstract

The high plasticity of root morphology, physiology, and function influences root-associated microbiomes. However, the variation in root-associated microbiome diversity and structures in response to root diameter at different root depths remains poorly understood. Here, we selected black locust (*Robinia pseudoacacia* L.) as a model plant to investigate the selection and network interactions of rhizospheric and root endophytic bacterial microbiomes associated with roots of different diameters (1, 1–2, and > 2 mm) among root depths of 0–100 cm via the Illumina sequencing of the 16S rRNA gene. The results showed that the alpha diversity of the root-associated bacterial communities decreased with increasing root diameters among different root depths; fewer orders with higher relative abundance, especially in the endosphere, were enriched in association with coarse roots (> 2 mm) than fine roots among root depths. Furthermore, the variation in the enriched bacterial orders associated with different root diameters was explained by bulk soil properties. Higher co-occurrence network complexity and stability emerged in the rhizosphere microbiomes of fine roots than those of coarse roots, in contrast to the situation in the endosphere microbiomes. In particular, the endosphere of roots with a diameter of 1–2 mm exhibited the lowest network complexity and stability and a high proportion of keystone taxa (e.g., Cytophagia, Flavobacteriia, Sphingobacteriia,  $\beta$ -Proteobacteria, and  $\gamma$ -Proteobacteria), suggesting a keystone taxon-reliant strategy in this transitional stage. In summary, this study indicated that root diameter at different root depths differentially affects rhizospheric and endophytic bacterial communities, which implies a close relationship between the bacterial microbiome, root function, and soil properties.

**Keywords** Root-associated bacterial microbiome · Root diameter · Root depth · Co-occurrence network

## Introduction

The rhizosphere is the interface between soil and plant roots, where beneficial microbes are recruited as the first

microbiological layer of plant defense [1], which protect the plants from pathogens and mediate plant development and nutrient cycling [2]. The endophytic bacteria living inside plant root tissue for all or part of their life cycle [3] are the second layer of plant defense [1]. Rhizospheric microorganisms are distributed heterogeneously in the rhizosphere because of differences in root traits (root morphology: primary or secondary, and root zones: root cap, lateral meristem, or border cells) [4]. The heterogeneity in the rhizosphere and endosphere creates microhabitats for diverse microbial taxa and facilitates beneficial interactions [5], which play critical roles in plant growth [6]. Therefore, it is imperative to clarify the heterogeneity of rhizospheric and endophytic microbiomes (root-associated microbiomes) to regulate plant growth by maximizing microbial function and root adaptation.

Root-associated microbiomes are largely influenced by the host plant and the soil environment [7]. Most recent studies have suggested that host plants provide multiple microhabitats

✉ Weimin Chen  
chenwm029@nwsuaf.edu.cn

<sup>1</sup> Shaanxi Key Laboratory of Agricultural and Environmental Microbiology, State Key Laboratory of Crop Stress Biology in Arid Areas, College of Life Sciences, Northwest A&F University, 3 Taicheng Road, Yangling, Xianyang 712100, Shaanxi, People's Republic of China

<sup>2</sup> Department of Microbiology, School of Basic Medical Sciences, Hubei University of Medicine, Shiyan 442000, Hubei, People's Republic of China

<sup>3</sup> Departamento de Microbiología, Escuela Nacional de Ciencias Biológicas, Instituto Politécnico Nacional, 11340 Mexico, D.F., Mexico

(e.g., plant compartments) for distinct microbial communities and affect the colonization of microbiomes [6–9]. Several other studies have demonstrated that the variation in host plant root traits also influences root-associated microbiomes. Szoboszlay et al. (2015) suggested that the wild maize ancestor (Balsas teosinte) and modern cultivars (sweet corn and popping corn) exhibit different root traits and harbor different rhizospheric microbiomes [10]. Pérez-Jaramillo et al. (2017) further analyzed the relationships between the rhizosphere microbiome and root traits of wild and domesticated *Phaseolus vulgaris* and indicated that wild bean accessions have thin roots whereas modern accessions have thick roots. Furthermore, Bacteroidetes were found to be dominant in wild bean accessions, while Verrucomicrobia and Actinobacteria occurred at higher relative abundance in modern bean accessions [11]. Saleem et al. (2018) suggested that fine roots, rather than primary and secondary root, recruit OTUs belonging to specialist organisms (the relative abundance of OTUs changes from fine to primary roots), which are mostly present at a relatively high abundance [5]. Fine roots with different branch orders also exhibit significantly different root-associated bacterial communities in poplar (*Populus × euramericana* (Dode) Guinier.) [12]. Even the root traits of first-order roots with different root diameters from various plant species vary significantly across the sequence of tropical, temperate, and desert biomes. Root diameter has the strongest effect on root traits. Compared with finer first-order roots, thicker first-order roots are more dependent on mycorrhizae [13]. These studies indicate that root diameter plays an important role in the composition of root-associated bacterial or fungal communities in different plant types at a local or global scale. Actually, based on root diameter, plant roots with < 1 or 2 mm and > 2 mm diameter are, respectively, classified as fine and coarse roots [14]. Fine roots are markedly different from coarse roots in terms of their morphology, nutrient concentrations, and functions. Fine roots are mainly distributed in the surface soil and exhibit high bioactivity, a large specific surface area, high nitrogen (N) concentrations [15], and a strong decomposition ability, all of which contribute to the soil carbon (C) flow and N cycling [16, 17]. Conversely, coarse roots, which exhibit rather low levels of bioactivity, are less efficient in absorbing soil nutrients [18]. Cregger et al. (2018) reported the fine (< 2 mm) and coarse (~ 5–20 mm) root-associated microbiomes of two genotypes of *Populus*. However, the differences in the community between fine and coarse roots were not specifically addressed in that study [9]. Overall, it is unclear how the root-associated bacterial community varies specifically between fine and coarse roots. On the other hand, plant roots exhibit a heterogeneous distribution in the soil in response to patchy and dynamically changing resources such as water and nutrients [19]. In vertical soil profiles, soil physicochemical properties differ significantly with depth in various ecosystems, and this causes variations in soil microbiome

[20–24]. Previous studies also indicate that the root-associated microbiome is influenced by soil types and properties [7, 12, 25]. Thus, soil properties may affect root traits, resulting in differences in root-associated bacterial communities. However, the variation in root-associated bacterial microbiomes among different root diameters across different soil depths, and the effect of soil properties on them, remains poorly understood.

As mentioned above, root traits and root-associated bacterial or fungal communities vary among different plant types. However, this is a limitation of the relationship between the root system and root-associated microbiome of leguminous tree species. Black locust (*Robinia pseudoacacia* L.) is an N-fixing leguminous tree species that increases soil N levels and enhances nitrification and N mineralization in soil via symbiotic N fixation with rhizobia, in turn promoting plant growth in poor or degraded soils [26, 27]. In addition, *Robinia pseudoacacia* (*R. pseudoacacia*) is used for soil rehabilitation [28]. In the present study, we selected *R. pseudoacacia* as a model plant and aimed (1) to investigate the effect of root diameter on the diversity and compositional variation of root-associated bacterial microbiomes (rhizospheric and root endophytic bacterial communities) and whether those are affected by root depth and (2) to explore whether the variation in the bacterial communities at different root diameters with root depth is affected by differences in soil properties via Illumina sequencing of the 16S rRNA gene. We hypothesized that root diameter would affect the root-associated bacterial microbiome of *R. pseudoacacia* L., and this would vary with root depth.

## Materials and Methods

**Sampling Location and Methods** Sampling was conducted on August 26–29, 2018, in Ansai County, Yan’an City, Shaanxi Province, China (108°51′44″–109°26′18″ E, 36°30′45″–37°19′31″ N). The area is located in the hinterland of the Loess Plateau and is characterized by vast *R. pseudoacacia* plantations. In general, *R. pseudoacacia* is in the early growth stage from April to June and the late growth stage from August to October. The period after the early growth stage and before the late growth stage is the accelerating growth stage [29]. We sampled in the late growth stage of *R. pseudoacacia*.

Three plots (each 10 × 10 m) were selected in the study area. The plots were spaced 5–10 m apart to preclude interactions. In each plot, three approximately 10-year-old trees of similar height and diameter at breast height were selected at random (Table S1). For each tree, soil samples and root samples were collected at a 50-cm distance from the trunk in a 100-cm-long vertical profile. The soil surrounding the plant roots (bulk soil) was collected from four soil depths (SD1, 0–

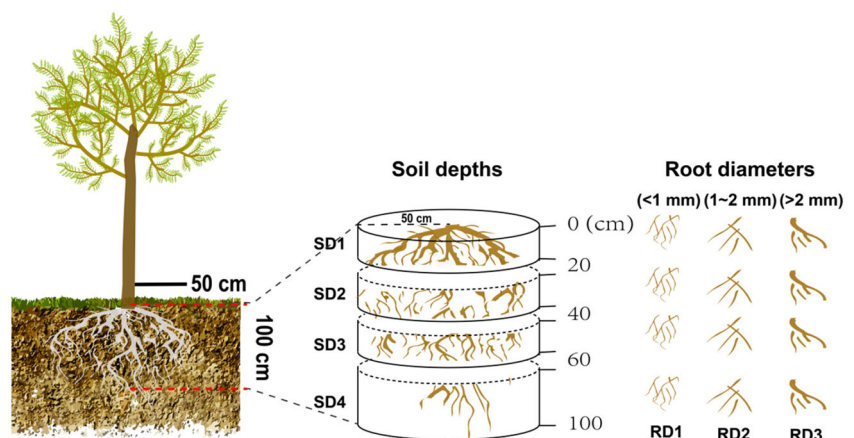
20 cm; SD2, 20–40 cm; SD3, 40–60 cm, and SD4: 60–100 cm) and passed through a 2-mm sieve [12]. All collected samples were placed in boxes with ice packs and transported back to the laboratory at  $-20^{\circ}\text{C}$ . A bulk soil subsample was used to analyze the soil physicochemical properties, including pH, organic matter (OM), total phosphorus (TP), total nitrogen (TN), total potassium (TK), total carbon (TC), nitrate nitrogen ( $\text{NO}_3^-$ -N), ammonium nitrogen ( $\text{NH}_4^+$ -N), available phosphorus (AP), and available potassium (AK) (Table S2, Supplementary materials) via routine methods [30]. The remaining subsample used for DNA analysis was stored at  $-80^{\circ}\text{C}$ . The living roots were picked from the soil and grouped based on root diameter (RD1,  $\leq 1$  mm; RD2, 1–2 mm; and RD3,  $> 2$  mm) and root depth (SD1, 0–20 cm; SD2, 20–40 cm; SD3, 40–60 cm; and SD4, 60–100 cm; Fig. 1). Rhizospheric soils were obtained by washing the roots, while the root samples designated for the endophyte analyses were cleaned and sonicated to eliminate rhizoplane microbes [7]. In total, 252 samples were obtained, including 36 bulk soil samples (9 replicates  $\times$  4 root depths) + 108 rhizospheric soil samples (9 replicates  $\times$  3 root diameters  $\times$  4 root depths) + 108 root samples (9 replicates  $\times$  3 root diameters  $\times$  4 root depths). The rhizospheric soil samples and root samples used for DNA analysis were stored at  $-80^{\circ}\text{C}$ .

**DNA Extraction and High-Throughput Sequencing** The extraction of metagenomic DNA from the bulk and rhizospheric soil samples (each 0.5 g) was performed using a FastDNA@ SPIN Kit for Soil (MP Biomedicals, Solon, USA) according to the manufacturer's instructions. Root samples (each 0.2 g) were pre-chilled with liquid nitrogen, and then ground using a mortar and pestle before metagenomic DNA extraction using a DNeasy Power Plant@ Pro-Kit (Qiagen GmbH, Hilden, Germany). The DNA concentrations and purity were determined using a NanoDrop 2000 UV-Vis spectrophotometer (Thermo Scientific, Wilmington, USA). DNA quality was checked by electrophoresis in a 1% (*w/v*) agarose gel.

The hypervariable V4–V5 region of the bacterial 16S rRNA gene was amplified using the 515F (5'-GTG CCA GCM GCC GCGG-3')/907R (5'-CCG TCA ATT CMT TTR AGT TT-3') primer pair (Jiao et al. 2016). PCR amplification was performed in a GeneAmp PCR system 9700 (ABI, Foster City, USA). PCR was performed in 20- $\mu\text{L}$  triplicate mixtures, each containing 4  $\mu\text{L}$  of 5 $\times$  FastPfu Buffer, 2  $\mu\text{L}$  of 2.5 mM dNTPs, 0.8  $\mu\text{L}$  of each primer (5  $\mu\text{M}$ ), 0.4  $\mu\text{L}$  of FastPfu Polymerase, 0.2  $\mu\text{L}$  of bovine serum albumin, 10 ng of template DNA, and double-distilled  $\text{H}_2\text{O}$ . The PCR conditions were as follows: initial denaturation at  $95^{\circ}\text{C}$  for 3 min; followed by 29 cycles of denaturation at  $95^{\circ}\text{C}$  for 30 s, annealing at  $55^{\circ}\text{C}$  for 30 s, and extension at  $72^{\circ}\text{C}$  for 45 s; and a final extension step at  $72^{\circ}\text{C}$  for 10 min. The PCR products were extracted from a 2% (*w/v*) agarose gel after electrophoresis. Further purification and quantification were performed using an AxyPrep DNA Gel Extraction Kit (Axygen Biosciences, Union City, USA) and a QuantiFluor<sup>TM</sup>-ST Fluorometer (Promega, Fitchburg, USA) according to the manufacturers' instructions. The purified amplicons were pooled in equimolar amounts and subjected to paired-end sequencing (2  $\times$  300 bp) on the Illumina MiSeq platform (Illumina, San Diego, USA) at Majorbio (Shanghai, China).

Raw FASTQ files were quality filtered using QIIME v1.9.1 [6] and merged using FLASH v1.2.11 [31]. The filtering criteria were as follows: (i) reads were truncated at any site receiving an average quality score  $< 20$  over a 50-bp sliding window; (ii) only sequences with overlap of greater than 10 bp were merged according to their overlap sequence with mismatches of no more than 2 bp; and (iii) the sequences of each sample were separated according to barcodes (exactly matching) and primers (allowing two nucleotide mismatches), and those containing ambiguous bases were removed [31]. Operational taxonomic units (OTUs) were clustered at a 97% similarity threshold using UPARSE v7.1 (<http://drive5.com/uparse/>) with a novel 'greedy' algorithm adopted to perform chimera filtering and OTU clustering simultaneously [32]. The

**Fig. 1** Schematic illustration of the experimental design for exploring the response of root-associated bacterial communities to root architecture in *R. pseudoacacia*. We sampled the soil within 50 cm of the tree trunk. RD1, RD2, and RD3 denote root diameters of  $< 1$  mm, 1–2 mm, and  $> 2$  mm, respectively. SD1, SD2, SD3, and SD4 represent root depths of 0–20 cm, 20–40 cm, 40–60 cm, and 60–100 cm, respectively



taxonomy of each 16S rRNA gene sequence was analyzed using the RDP Classifier (<http://rdp.cme.msu.edu/>) against the Silva 16S rRNA database (Release 128; <http://www.arb-silva.de/>) with a confidence threshold of 70% [33].

**Statistical Analysis** All data were normalized using the trimmed mean of  $M$  value method for subsequent analyses [6]. Alpha-diversity indices (Shannon index and OTU richness) were calculated to assess bacterial diversity and species richness. To estimate bacterial beta diversity, the Bray–Curtis distances between rhizosphere or root samples were calculated with the `vegdist()` function of the R package “vegan” (version 2.5-6), and the compositional differences in bacterial communities were then visualized through principal coordinate analysis (PCoA) with the “ape” (version 5.3) package in R (v3.5.2; <http://www.r-project.org/>) [34]. The variation in bacterial beta diversity was examined through analysis of similarities (ANOSIM) and permutational multivariate analysis of variance (PERMANOVA, also known as ADONIS) based on the Bray–Curtis similarity matrix using the “vegan” package in R [20].

Kruskal–Wallis tests and Wilcoxon tests (Mann–Whitney  $U$  test) were performed using the “ggpubr” (version 0.2.3) package in R for multiple comparisons and pairwise comparisons, respectively.  $P$  values were adjusted by using the Benjamini and Hochberg false discovery rate (FDR) test [35], and the adjusted  $P$  values had a cutoff of 0.05. Two-way analysis of variance (ANOVA) was used to compare the effects of root diameter, root depth, and the interaction of the two terms on alpha-diversity in the rhizosphere and the endosphere; analysis was performed using “HH” (version 3.1-42) package [36]. The OTUs that were significantly enriched in the rhizosphere and endosphere for each root diameter were presented in ternary plots with the “ggtern” (version 3.1.0) package in R [20]. Bar plots were constructed using the “vcd” (version 1.4.4) package in R to display the proportions of the ten most abundant bacterial orders based on the enriched OTUs for each root diameter at different depths. SourceTracker (v.1.0) based on the Bayesian approach was used to estimate the sources of the root-associated microbiome with coarse roots or deep soil layers [37]. Redundancy analysis (RDA) of the correlation between soil properties (significance at  $P < 0.05$ , through constrained axis variance test using version 4.0.2 “stats” package) and ten enriched root-associated bacterial orders was generated using the “vegan” package in R [38].

A co-occurrence network was constructed based on strong (Spearman’s  $\rho > 0.7$ ) significant ( $P$  value  $< 0.05$ ) correlations to explore the interactions between OTUs with a relative abundance  $\geq 0.01\%$ . In detail, statistical analyses were performed in the R environment with the “igraph” (version 1.2.4.1) package to calculate network topological features,

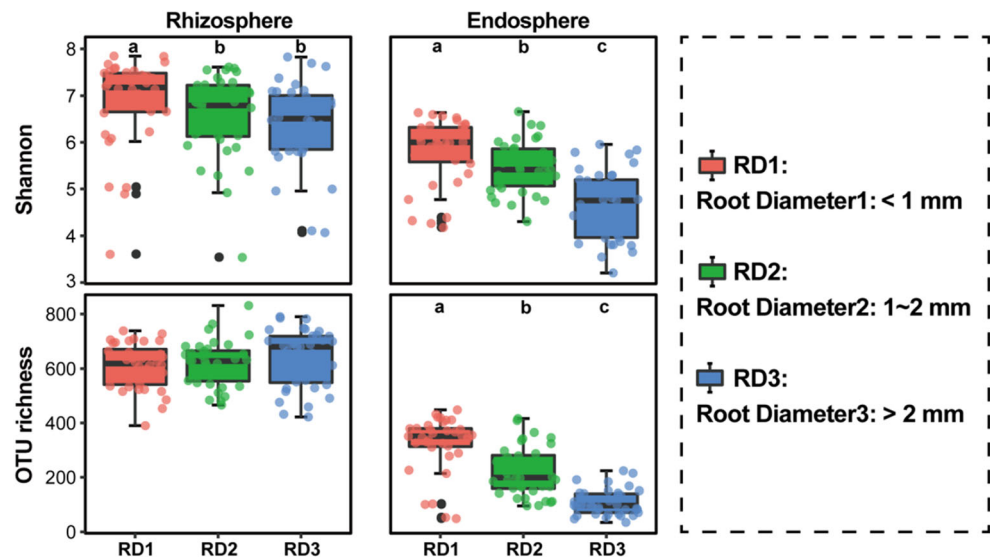
including the node number, edge number, average degree, diameter, density, modularity, average clustering coefficient, and average path length [39]. In addition, the “Hmisc” (version 4.2-0) package was used to calculate the correlation matrix (Spearman correlation coefficient values) and the significance matrix ( $P$  value). The co-occurrence network was visualized in Gephi (<https://gephi.org/>) [39]. The taxonomic classification of bacteria in the network modules of the rhizosphere and endosphere (RD1 to RD3) was plotted using Krona (<https://github.com/marbl/Krona/wiki>) [40]. In addition, the  $z$ -score and  $c$ -score were calculated for each node according to the methods of metabolic networks [41]. Nodes with a  $z$ -score  $> 2.5$  were classified as hubs, and nodes with a  $z$ -score  $< 2.5$  were classified as nonhubs. Based on  $c$ -scores, network hubs ( $z$ -score  $> 2.5$ ;  $c$ -score  $> 0.6$ ) and module hubs ( $z$ -score  $> 2.5$ ;  $c$ -score  $< 0.6$ ) were defined, whereas nonhubs were classified as connectors ( $z$ -score  $< 2.5$ ;  $c$ -score  $> 0.6$ ) and peripherals ( $z$ -score  $< 2.5$ ;  $c$ -score  $< 0.6$ ). Network hubs, module hubs, and connectors were designated keystone taxa with connective functions in the network. The natural connectivity and average degree after the removal of nodes in the static network were used to estimate network stability. They reflected the sensitive variation of network structural robustness and were used to assess network robustness [42].

## Results

### Diversity and Composition of Root-Associated Microbiomes

In total, 3,634,858 high-quality bacterial sequences and 2083 OTUs were obtained across all samples after normalization. The Shannon index of rhizospheric bacterial communities was significantly different between RD1 and RD2 ( $P = 0.042$ ) and between RD1 and RD3 ( $P = 0.004$ ), while no significant differences were observed in their OTU richness among the three root diameters (Fig. 2). The Shannon indices of rhizospheric bacterial communities were not significantly different among the three root diameters across the four root depths (Fig. S1a). The endophytic bacterial communities differed significantly in terms of their alpha-diversity indices among various root diameters (Fig. 2), although the alpha-diversity indices of the endophytic bacterial communities were not significantly different between RD1 and RD2 at root depths SD1 and SD2 (Fig. S1a). Two-way ANOVA also showed that the alpha diversity of the root-associated bacterial microbiome and the rhizospheric bacterial microbiome was influenced mainly by root diameter (Shannon index,  $P < 0.001$ ; OTU richness,  $P < 0.05$ ) and root depth (Shannon index,  $P < 0.01$ ; OTU richness,  $P < 0.001$ ), respectively. And the Shannon index of the bacterial microbiome in endosphere was influenced mainly by root diameter ( $P < 0.001$ ), while the OTU richness was

**Fig. 2** Shannon index and operational taxonomic unit (OTU) richness of bacterial communities in the rhizosphere and root endosphere of *R. pseudoacacia* among different root diameters visualized using boxplots. Data are the mean  $\pm$  standard deviation ( $n = 36$ ). Different letters above the columns indicate significant differences between groups ( $P < 0.05$ )



influenced by both root diameter ( $P < 0.001$ ) and depth ( $P < 0.05$ ; Table S2). These results indicated that the alpha diversity of the root-associated bacterial communities decreased significantly with an increase in root diameter, especially the endophytic community, which exhibited similar changes with root depth. Moreover, root depth and diameter differently affected the bacterial diversity of the rhizosphere and the endosphere.

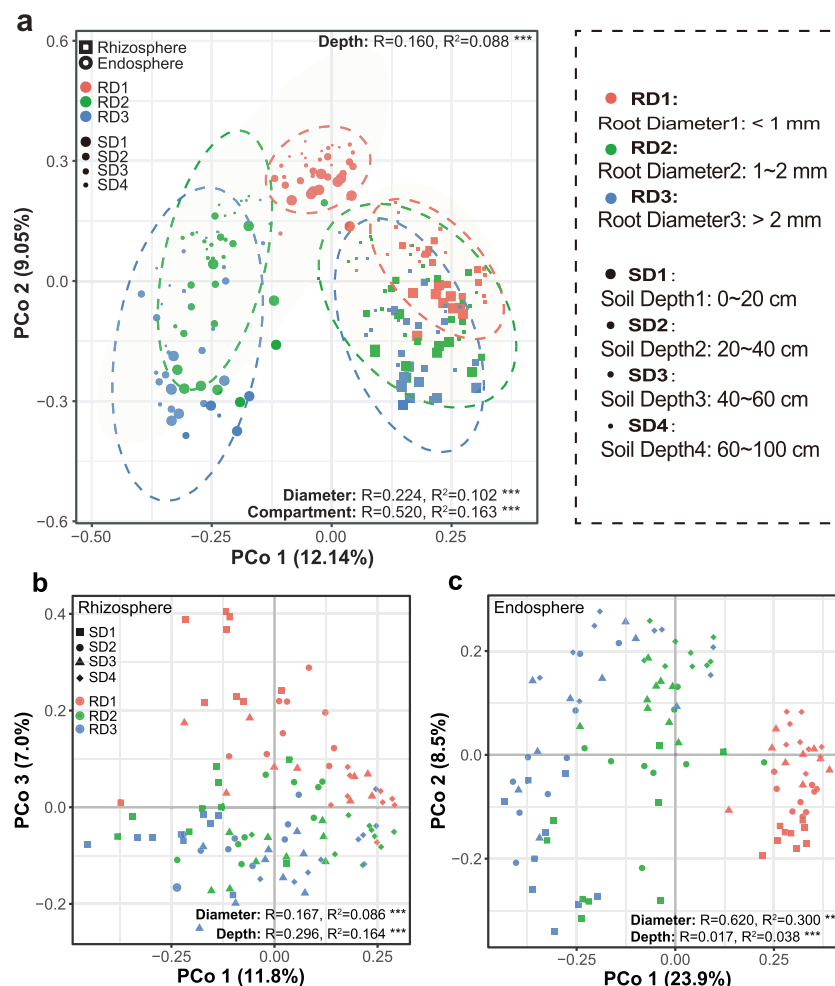
With regard to beta diversity, the Bray–Curtis distance-based PCoA revealed that the rhizosphere and root samples generated clearly different clusters in the ordination plot. Statistically, the root compartment explained the greatest amount of the variation in the bacterial communities (compartment: ANOSIM  $R = 0.520$ , ADONIS  $R^2 = 0.163$ ,  $P < 0.001$ ). In addition, we observed significant compositional differences in both the rhizospheric and endophytic bacterial communities across various root diameters and depths (diameter:  $R_{\text{ANOSIM}} = 0.224$ ,  $R^2_{\text{ADONIS}} = 0.102$ ,  $P < 0.001$ ; depth:  $R_{\text{ANOSIM}} = 0.160$ ,  $R^2_{\text{ADONIS}} = 0.088$ ,  $P < 0.001$ ; Figs. 3a and S2). For the rhizospheric bacterial communities, the analysis of similarity (ANOSIM) and permutational multivariate analysis of variance (PERMANOVA, also known as ADONIS) indicated significant differences in the microbial communities across root diameters and depths (diameter:  $R_{\text{ANOSIM}} = 0.167$ ,  $R^2_{\text{ADONIS}} = 0.086$ ,  $P < 0.001$ ; depth:  $R_{\text{ANOSIM}} = 0.296$ ,  $R^2_{\text{ADONIS}} = 0.164$ ,  $P < 0.001$ ; Fig. 3b). For endophytic bacterial communities, the greatest separation between the microbial communities was associated with the root diameter ( $R_{\text{ANOSIM}} = 0.620$ ,  $R^2_{\text{ADONIS}} = 0.300$ ,  $P < 0.001$ ), and the second largest source of variation was root depth ( $R_{\text{ANOSIM}} = 0.017$ ,  $R^2_{\text{ADONIS}} = 0.038$ ,  $P < 0.001$ ; Fig. 3c). The results indicate that the composition of root-associated bacterial communities differed significantly among the various root diameters and depths.

**Relationship Between the Enriched Taxa with Different Root Diameters and Soil Properties** The significantly enriched OTUs and the ten most abundant bacterial orders based on different root diameters were displayed using ternary plots and bar plots (Fig. 4). The lowest numbers of enriched OTUs were recorded for RD2 in both the rhizosphere (55) and the endosphere (61). The numbers of enriched OTUs increased to 173 and 258 in the rhizosphere of RD1 and RD3, respectively, while 618 and 198 enriched OTUs were observed in the endosphere of RD1 and RD3, respectively (Fig. 4a).

Among the enriched bacterial taxa, Rhizobiales was dominant at all root diameters in the rhizosphere and the endosphere. Burkholderiales and Rhizobiales were the most dominant taxa in RD1 of the rhizosphere and the endosphere, respectively, while Rhodospirillales and Rhizobiales were the most dominant taxa in RD2 and RD3, respectively. Additionally, RD3 of the rhizosphere showed a more even community structure compared with RD1 (Figs. 4a and S3), indicating the selection effect of the specific bacterial order in RD3 (Figs. 4a and S3). The most dominant bacterial orders across different root depths were similar, although the relative abundance exhibited variation (Fig. S3).

The ten enriched orders were used for correlation analysis with soil properties. The RDA biplot showed that the variances of bacterial communities in all root diameters at shallower soil depths (SD1 and SD2) were explained by AK. AK and OM were positively correlated with Burkholderiales, and AP was positively correlated with Rhizobiales in RD1 of the rhizosphere. TC and OM explained the bacterial variance in the rhizosphere or endosphere of other root diameters. Interestingly, the correlation between Rhizobiales and AK changed from negative to positive with increasing root diameter (Fig. 4b). These results indicated that

**Fig. 3** Principal coordinate analysis based on the Bray–Curtis distance of bacterial communities in the rhizosphere and root endosphere of *R. pseudoacacia*. Community composition based on the root compartment (rhizosphere and endosphere), root diameter, and root depth (a). Root diameter and root depth are presented simultaneously as the variables influencing rhizospheric (b) and endophytic communities (c)



specific bacterial orders associated with different diameters across root depths were affected differently by soil properties. The correlations between the enriched bacterial orders and soil properties in RD2 and RD3 were similar.

#### Co-occurrence Network Interactions of Root-Associated Microbiomes Among Root Diameters Across Depths

In the co-occurrence network of rhizospheric bacterial communities, the node number, edge number, network density, and average clustering coefficient all decreased with an increase in the root diameter. Among the endophytic bacterial communities, increases in the network topological feature values occurred in the order of  $RD3 > RD1 > RD2$  and  $SD4 < SD3 < SD2 < SD1$  (Table S4). The similar trends were found in network complexity in the rhizosphere and the endosphere (Figs. 5a and S5). A total of 274 shared nodes were found in the rhizospheric networks (Fig. 5b), while only 13 shared nodes were observed in the endophytic networks across the three root diameters (Fig. 5c). These results indicated that the diversity of the rhizospheric microbiome was more similar among different root diameters than that of the

endospheric microbiome, which agreed with the alpha and beta diversity results.

The network nodes for the rhizospheric and endophytic taxa at the OTU level were classified into network hubs, module hubs, connectors, and peripherals based on  $z$ -scores and  $c$ -scores (Fig. 5d). At the class level, members of the phylum Chloroflexi were the keystone taxa in both the rhizosphere (Anaerolineae and Thermomicrobia for both RD2 and RD3) and the endosphere (Chloroflexi for both RD1 and RD2). Similarly, Rhizobiales were observed as keystone taxa in the rhizosphere (RD2 and RD3) and endosphere (RD1 and RD2). In addition, members of the phyla Bacteroidetes (Cytophagia, Flavobacteriia, and Sphingobacteriia),  $\beta$ -Proteobacteria, and  $\gamma$ -Proteobacteria were keystone taxa in the endosphere (RD2; Fig. 5e). Therefore, the rhizospheric and endospheric microbiomes associated with different root diameters exhibit different keystone taxa.

Different modules of the co-occurrence network harbored various taxa. Among the major modules of the rhizospheric network, Rhizobiales, Burkholderiales, Planctomycetales, Xanthomonadales, Sphingobacteriales, and Rhodospirillales were ubiquitous among several modules and root diameters

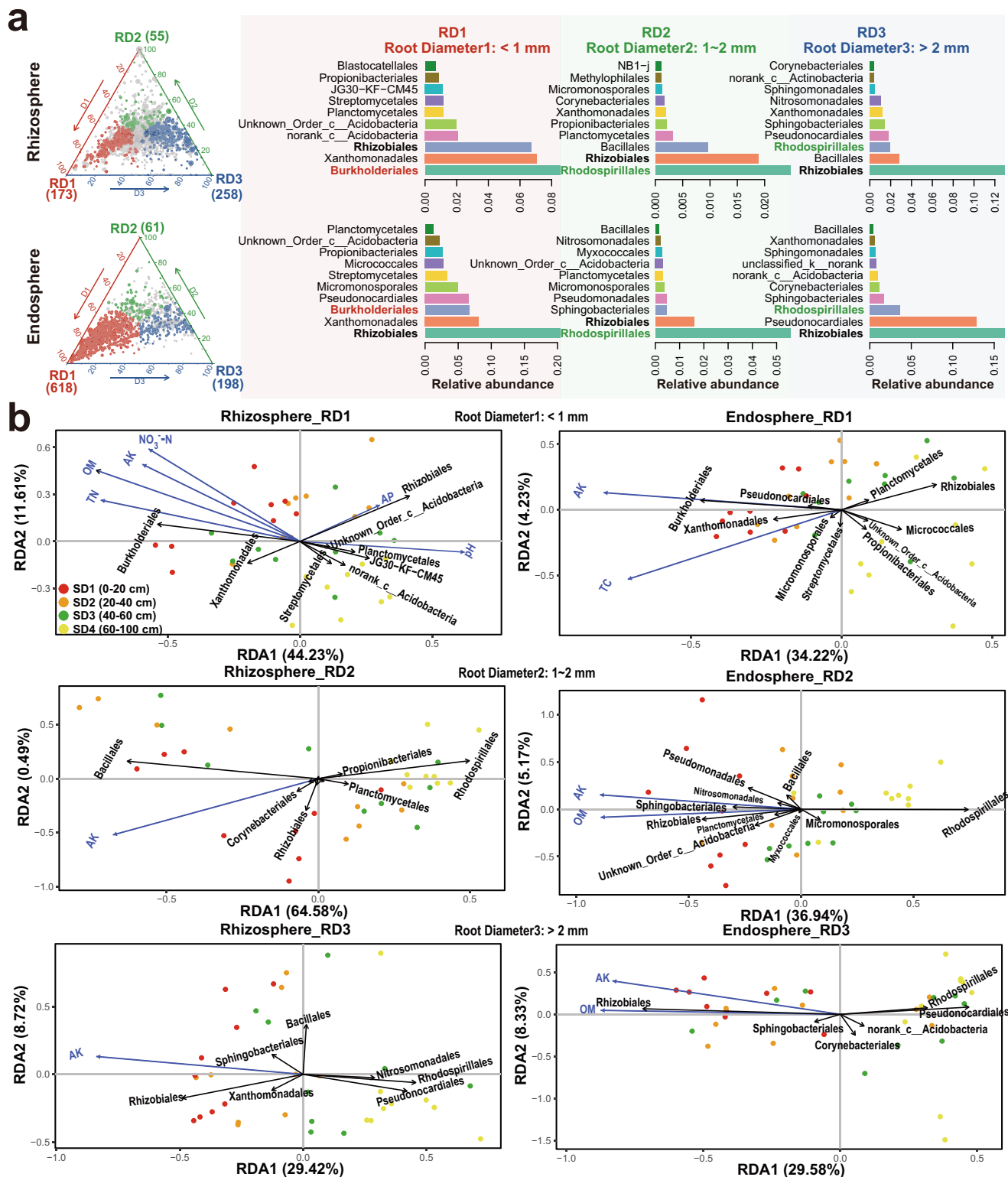


**Fig. 4** Ternary plots (a) showing the significantly enriched OTUs in the rhizosphere and roots with different root diameters. The colors indicate the different root diameters. The size of each circle represents the relative abundance. The varying numbers of OTUs are indicated at the vertices of the ternary plots. The ten most abundant orders based on significantly

enriched OTUs are displayed in bar plots. Redundancy analysis (RDA; b) showing the correlation among bacterial communities and soil properties. Soil properties were selected through constrained axis variance test ( $P < 0.05$ )

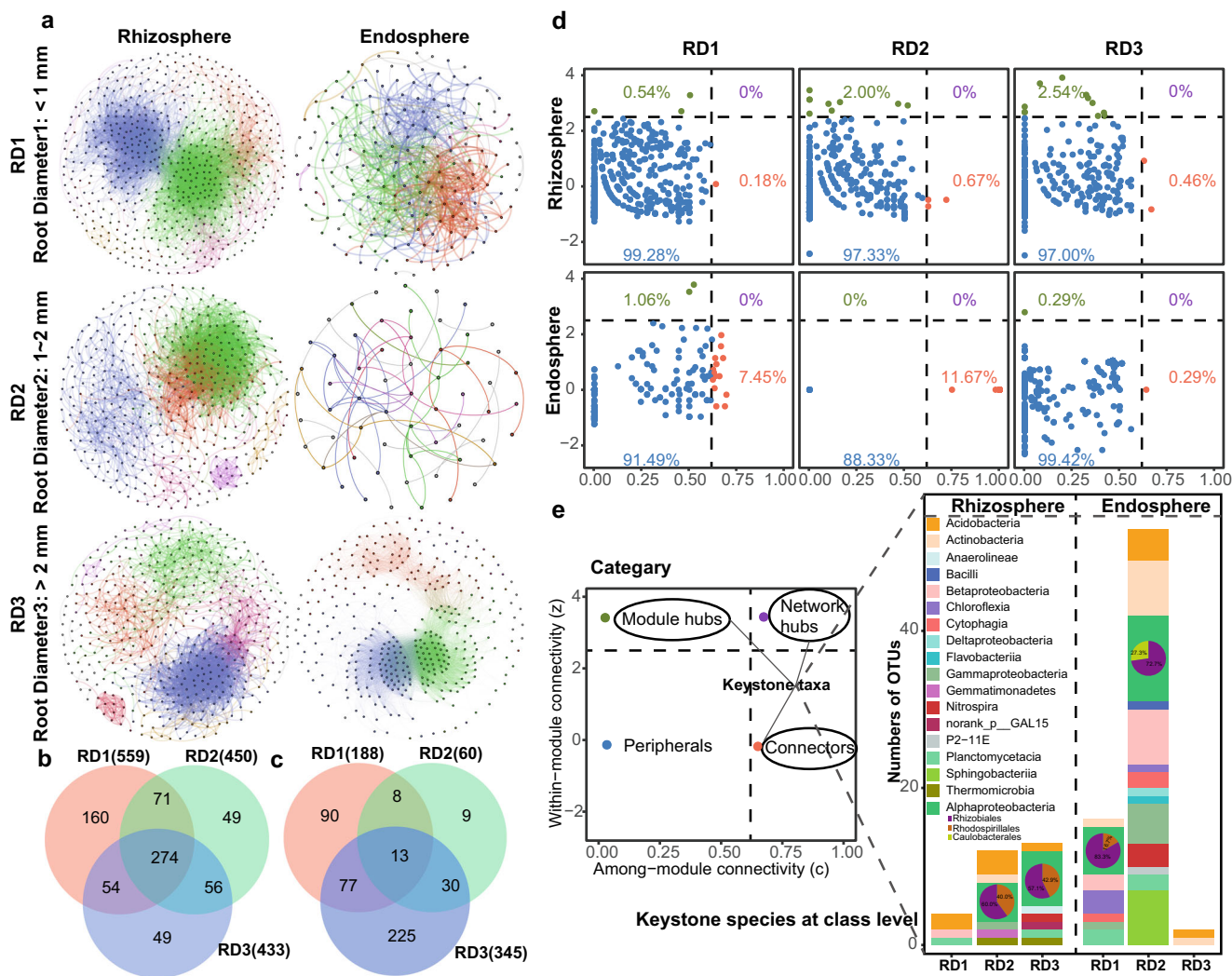


**Fig. 5** Co-occurrence networks of *R. pseudoacacia* root-associated bacterial communities among different root diameters (**a**) and the numbers of all nodes in the networks of the rhizosphere (**b**) and root endosphere (**c**). Each point represents a selected OTU with a relative abundance  $\geq 0.01\%$ . Strong (Spearman's  $\rho > 0.7$ ) significant (false discovery rate-corrected  $P$  value  $< 0.05$ ) correlations between the nodes are selected. The colors

(Fig. S6a–c). The proportions of Gaiellales and Propionibacteriales increased with an increase in the root diameter, while the proportions of Rhizobiales were relatively low in the endosphere of coarse roots (Figs. 4 and S6f). In addition, modules consisting mainly of Bacillales were observed in the rhizospheric networks of RD2 (Module 21) and RD3 (Module 7), and modules consisting mainly of Burkholderiales and Pseudomonadales were found in the rhizospheric networks of RD2 (Module 1) and RD3 (Module 1). Similar to the rhizospheric taxa, various endophytic taxa, including Rhizobiales, Burkholderiales, Bacillales, and Pseudomonadales, were also ubiquitous in RD1, RD2, and RD3 (Fig. S6d–f). In addition, Desulfurellales in Module 11 of the RD3 endophytic network was unique.

represent different modules distributed randomly. Network module features at the OTU level for rhizospheric and root endophytic communities, including network hubs, module hubs, connectors, and peripherals (**d**). Higher taxonomic levels corresponding to network hubs, module hubs, and connectors based on OTUs (**e**)

The keystone taxa with the lowest proportions and the highest average degree and natural connectivity were found in the RD1 rhizosphere and the RD3 endosphere, which were the two root diameters exhibiting the highest network complexity and stability (Figs. 5e and S7; Table S4). In contrast, the average degree and natural connectivity were lowest in the RD2 endosphere (Fig. S7). Additionally, the co-occurrence network was less complex than that of RD1 and RD3 according to the topological features. These results indicated that the network of the RD2 endosphere was the most unstable, which resulted in the lowest ability to enrich bacterial taxa in RD2 (Figs. 4 and S4), and revealed that RD2 in the transitional stage from fine to coarse roots exhibited the lowest resistance to maintaining stable interactions between bacteria.



Taken together, the co-occurrence network patterns, including the network complexity and stability and the bacterial community composition of the rhizosphere and the endosphere, were affected by root diameter, which also varied across root depths.

## Discussion

In the present study, we investigated the effects of root diameter among root depths on the rhizospheric and endophytic bacterial microbiomes of *R. pseudoacacia*. According to the results, the root-associated bacterial microbiomes were influenced by root diameter, and this varied across root depths due to the variation in soil properties. The influence was particularly evident with respect to bacterial diversity, the taxonomic composition, the correlation between enriched bacterial orders and soil properties, and co-occurrence patterns.

**The Effect of Root Diameter Among Root Depths on Root-Associated Bacterial Diversity** Bacterial diversity was lower in association with the coarse roots than the fine roots of *R. pseudoacacia*. Consistent with these results, larger-diameter roots, whether classified by root order [12] or morphology [5], were associated with lower bacterial diversity. This could be linked to the much greater surface area of fine roots than coarse roots, and the much higher levels of nutrients and metabolites associated with fine roots may consequently increase microbial diversity [5]. In contrast, coarse roots, with lower nutrient levels [15], could lead to P limitation, restricting the growth of both plants and microbes [43]. This could also be related to the variation in the turnover between fine roots and coarse roots [16, 17]. For example, fine roots have a short life span that could result in strong root decomposition, which is believed to serve as a potential soil C source. The traits of fine roots could cause the recruitment of more diverse bacterial taxa. However, coarse roots, which have a slow turnover of C and nutrients as well as a more structural function and more lignified composition, could restrict the growth of certain groups of microorganisms [16, 17].

The variation in root-associated bacterial diversity among root diameters differed in root-associated compartments (rhizosphere and endosphere; Figs. 2 and 3 and S1). Bacterial diversity in the rhizosphere was more affected by root depth than that in the endosphere, suggesting that the soil environment played a larger role in rhizospheric bacterial diversity as rhizosphere is an extended root phenotype to forage soil nutrient [19], which was consistent with the report by Xiao [7]. Differently, the present study provides a new perspective regarding the variation of root diameter in root-associated bacterial microbiomes in root-associated compartments as well as a better understanding of root-associated

compartment selection effects on root-associated bacterial microbiomes.

## The Different Filtering Effects of Fine and Coarse Roots on Root-Associated Bacterial Microbiomes Linked to Root Functional Traits and Soil Properties

In our study, along the root diameter trajectory from fine to coarse, we observed that most of the enriched bacterial orders associated with different root diameters belonged to Proteobacteria and Actinobacteria, whereas these groups (particularly Rhizobiaceae and Nocardioideae) were reported to be more strongly associated with thicker roots in the rhizosphere of modern common bean [11]. Similar to Pérez-Jaramillo et al. (2017), we observed that the Rhizobiales with higher relative abundance occurred in the rhizosphere and the endosphere associated with various root diameters, suggesting that the symbiotic N-fixing system of the legumes *R. pseudoacacia* [26] and *Phaseolus vulgaris* [11] is linked to the recruitment of Rhizobiales. Intriguingly, the variation in Rhizobiales with increasing root diameter was linked to AK and AP in the present study. Previous studies have indicated that symbiotic nitrogen fixers belonging to Rhizobiales have also shown K and P solubilizing activity [44]. The correlation between Rhizobiales and AP in RD1 of the rhizosphere could imply a larger demand for P in the bacterial community with higher diversity [43] compared with RD2 and RD3. The efficiency of K-solubilization by microorganisms is improved by lowering pH and is affected by oxygen [44]. Consistently, in this study, AK was correlated negatively with pH and explained the variance of root-associated bacterial communities at shallower depths. Rhodospirillales was found to have the potential to contribute to the N uptake of plants [45]. Thus, its dominance in RD2 and RD3 associated with deeper root depth could compensate for the lower capacity for nutrient acquisition of coarse roots and the lower N content in deeper soil layers. Analogous to the complementary relationship between mycorrhizal fungi and plant roots: thin roots forage nutrients independently, while thick roots rely on their associated mycorrhizal fungi [46].

Furthermore, compared with fine roots, the coarse roots in the rhizosphere were dominated by members of Gaiellales and Propionibacteriales (Fig. S6f), which can respond to low levels of flavonoids [47]. In turn, the rhizosphere microbiome assembly drives the systemically induced root exudation of metabolites via root-to-root signaling [48]. In this study, the root-associated bacterial microbiome was selected from the nearby root diameters or depths (Fig. S4), suggesting that root-to-root signaling could play an important role in filtering effect of root-associated microbiome. This is consistent with the view that selection means that particular species are dominant in an ecological community because of their functional traits [49]. These results indicate that the filtering effects of

roots on root-associated bacterial microbiomes are related to root functional traits and soil properties.

### Potential Strategies Depending on the Network Interactions of Root-Associated Bacterial Microbiomes

We observed that the RD1 networks exhibited the highest proportion of negative correlations (edges; rhizosphere: 8.56%; endosphere: 29.52%) compared with the RD2 (rhizosphere: 1.43%; endosphere: 0%) and RD3 networks (rhizosphere: 1.78%; endosphere: 0%; Table S4). In general, positive correlations indicate less competitive interactions and more mutualistic interactions [50]; thus, the potential for cooperative or syntrophic interactions was greater in coarse roots than in fine roots. This could be a strategy depending on the mutualistic interactions between bacterial taxa to compensate for the low absorption of nutrients in coarse roots, analogous to the reliance of thick roots on their associated mycorrhizal fungi [46].

On the other hand, the co-occurrence network of RD2 was less complex and stable than those of RD1 and RD3 (Figs. 5a and S7; Table S4), as RD2 is in a transitional stage from fine root to coarse root and has a high community turnover, which results in high stochasticity in species co-occurrences [51]. Consequently, the network keystone taxa in the RD2 endosphere (e.g., Cytophagia, Flavobacteriia, Sphingobacteriia,  $\beta$ -Proteobacteria, and  $\gamma$ -Proteobacteria; Fig. 5e) exhibited copiotrophic attributes, such as higher growth rates and lower substrate affinities [52], to adapt to the high community turnover. These results indicated that this could be a strategy relying on keystone taxa to maintain network stability in roots and thereby influence root functions. Further research into the factors affecting the assembly of the microbiome in the transitional stage could provide new evidence regarding the mechanisms underpinning root-microbe interactions. Taken together, the results demonstrated that the network interactions of root-associated bacterial microbiomes could be potential strategies whereby roots influence root functions.

## Conclusions

In the present study, we revealed that different root diameters among root depths affected both the rhizospheric and root endophytic bacterial microbiomes of *R. pseudoacacia*. The selection and network interactions of the bacterial community differed among root diameters across depths with root-associated compartments (rhizosphere and endosphere). The variation in root-associated compartments presented distinct response patterns to different root diameters among root depths. Although the rhizosphere soil properties of different root diameters were not measured, these results still demonstrated the relationship between root-associated bacterial microbiomes from root diameters across root depths and soil properties. The results implied that the recruitment and interactions of the specific root-associated bacterial

microbiome play critical roles in plant growth. Further studies are required to clarify the function of specific species selected by root niches and to achieve the maximization of microbial function and root adaptability by regulating the root-associated microbiome.

**Supplementary Information** The online version contains supplementary material available at <https://doi.org/10.1007/s00248-020-01678-4>.

**Funding** This study was supported by the National Natural Science Foundation of China (31870476 and 41830755).

**Data Availability** The raw sequence data reported in this paper are available in the NCBI Sequence Read Archive under BioProject PRJNA600550.

## Compliance with Ethical Standards

**Conflict of Interest** The authors declare that they have no conflict of interest.

## References

- Dini-Andreote F (2020) Endophytes: the second layer of plant defense. *Trends Plant Sci* 25(4):319–322. <https://doi.org/10.1016/j.tplants.2020.01.007>
- Chen YL, Palta JA, Wu PT, Siddique KHM (2019) Crop root systems and rhizosphere interactions. *Plant Soil* 439(1):1–5. <https://doi.org/10.1007/s11104-019-04154-2>
- Hardoim PR, van Overbeek LS, Elsas JDV (2008) Properties of bacterial endophytes and their proposed role in plant growth. *Trends Microbiol* 16(10):463–471. <https://doi.org/10.1016/j.tim.2008.07.008>
- Philippot L, Raaijmakers JM, Lemanceau P, van der Putten WH (2013) Going back to the roots: the microbial ecology of the rhizosphere. *Nat Rev Microbiol* 11(11):789–799. <https://doi.org/10.1038/nrmicro3109>
- Saleem M, Law AD, Sahib MR, Pervaiz ZH, Zhang Q (2018) Impact of root system architecture on rhizosphere and root microbiome. *Rhizosphere* 6:47–51. <https://doi.org/10.1016/j.rhisph.2018.02.003>
- Edwards J, Johnson C, Santos-Medelln C, Lurie E, Natarajkumar P, Bhatnagar S, Eisen J, Sundaresan V (2015) Structure, variation, and assembly of the root-associated microbiomes of rice. *PNAS* 112(8):E911–E920. <https://doi.org/10.1073/pnas.1414592112>
- Xiao X, Chen WM, Zong L, Yang J, Jiao S, Lin YB, Wang ET, Wei GH (2017) Two cultivated legume plants reveal the enrichment process of the microbiome in the rhizocompartments. *Mol Ecol* 26:26–1651. <https://doi.org/10.1111/mec.14027>
- Xiong C, Zhu YG, Wang JT, Singh B, Han LL, Shen JP, Li PP, Wang GB, Wu CF, Ge AH, Zhang LM, He JZ (2020) Host selection shapes crop microbiome assembly and network complexity. *New Phytol*. 229:1091–1104. <https://doi.org/10.1111/nph.16890>
- Cregger MA, Veach AM, Yang ZK, Crouch MJ, Vilgalys R, Tuskan GA, Schadt CW (2018) The *Populus* holobiont: dissecting the effects of plant niches and genotype on the microbiome. *Microbiome* 6(1):31. <https://doi.org/10.1186/s40168-018-0413-8>
- Szoboszlay M, Lambers J, Chappell J, Kupper JV, Moe LA, McNear DH (2015) Comparison of root system architecture and rhizosphere microbial communities of *Balsas* teosinte and domesticated corn cultivars. *Soil Biol Biochem* 80:34–44. <https://doi.org/10.1016/j.soilbio.2014.09.001>

11. Pérez-Jaramillo JE, Carrión VJ, Bosse M, Ferrão LFFV, de Hollander M, Garcia AAF, Ramírez CA, Mendes R, Raaijmakers JM (2017) Linking rhizosphere microbiome composition of wild and domesticated *Phaseolus vulgaris* to genotypic and root phenotypic traits. *ISME J* 11(10):2244–2257. <https://doi.org/10.1038/ismej.2017.85>
12. Wang QT, Wang N, Wang YP, Wang QK, Duan BL (2017) Differences in root-associated bacterial communities among fine root branching orders of poplar (*Populus × euramericana* (Dode) Guinier.). *Plant Soil* 421(1):123–135. <https://doi.org/10.1007/s11104-017-3449-9>
13. Ma ZQ, Guo DL, Xu XL, Lu M, Bardgett RD, Eissenstat DM, McCormack ML, Hedin LO (2018) Evolutionary history resolves global organization of root functional traits. *Nature* 555(7694):94–97. <https://doi.org/10.1038/nature25783>
14. Zhang XY, Wang W (2015) The decomposition of fine and coarse roots: their global patterns and controlling factors. *Sci Rep* 5(1):9940. <https://doi.org/10.1038/srep09940>
15. Yuan ZY, Chen H (2010) Fine root biomass, production, turnover rates, and nutrient contents in boreal forest ecosystems in relation to species, climate, fertility, and stand age: literature review and meta-analyses. *Crit Rev Plant Sci* 29(4):204–221. <https://doi.org/10.1080/07352689.2010.483579>
16. Endo I, Kume T, Kho LK, Katayama A, Makita N, Ikeno H, Ji I, Ohashi M (2019) Spatial and temporal patterns of root dynamics in a Bornean tropical rainforest monitored using the root scanner method. *Plant Soil*. 443:323–335. <https://doi.org/10.1007/s11104-019-04203-w>
17. Wang GL, Liu F, Xue S (2017) Nitrogen addition enhanced water uptake by affecting fine root morphology and coarse root anatomy of Chinese pine seedlings. *Plant Soil* 418(1):177–189. <https://doi.org/10.1007/s11104-017-3283-0>
18. Marsden C, Nouvellon Y, Epron D (2008) Relating coarse root respiration to root diameter in clonal Eucalyptus stands in the Republic of the Congo. *Tree physiol* 28:1245–1254. <https://doi.org/10.1093/treephys/28.8.1245>
19. de la Fuente Cantó C, Simonin M, King E, Moulin L, Bennett MJ, Castrillo G, Laplace L (2020) An extended root phenotype: the rhizosphere, its formation and impacts on plant fitness. *Plant J* 103(3):951–964. <https://doi.org/10.1111/tj.14781>
20. Jiao S, Chen WM, Wang JL, Du NN, Li QP, Wei G (2018) Soil microbiomes with distinct assemblies through vertical soil profiles drive the cycling of multiple nutrients in reforested ecosystems. *Microbiome* 6(1):146. <https://doi.org/10.1186/s40168-018-0526-0>
21. Wang YJ, Liu L, Tian YL, Wu XP, Yang JF, Luo Y, Li HK, Awasthi MK, Zhao ZY (2020) Temporal and spatial variation of soil microorganisms and nutrient under white clover cover. *Soil Tillage Res* 202:104666. <https://doi.org/10.1016/j.still.2020.104666>
22. Cai Y, Shen JP, Di HJ, Zhang LM, Zhang C, He JZ (2020) Variation of soil nitrate and bacterial diversity along soil profiles in manure disposal maize field and adjacent woodland. *J Soils Sed* 20(10):3557–3568. <https://doi.org/10.1007/s11368-020-02679-z>
23. Liu Y, Chen XT, Liu JX, Liu TT, Cheng JM, Wei GH, Lin YB (2019) Temporal and spatial succession and dynamics of soil fungal communities in restored grassland on the Loess Plateau in China. *Land Degrad Dev* 30(11):1273–1287. <https://doi.org/10.1002/ldr.3289>
24. Liang XL, Wagner RE, Zhuang J, DeBruyn JM, Wilhelm SW, Liu F, Yang L, Staton ME, Sherfy AC, Radosevich M (2019) Viral abundance and diversity vary with depth in a southeastern United States agricultural ultisol. *Soil Biol Biochem* 137:137. <https://doi.org/10.1016/j.soilbio.2019.107546>
25. Liu LL, Huang X, Zhang JB, Cai ZC, Jiang K, Chang YY (2020) Deciphering the relative importance of soil and plant traits on the development of rhizosphere microbial communities. *Soil Biol Biochem* 148:107909. <https://doi.org/10.1016/j.soilbio.2020.107909>
26. Bolat İ, Kara Ö, Sensoy H, Yüksel K (2016) Influences of black locust (*Robinia pseudoacacia* L.) afforestation on soil microbial biomass and activity. *iForest* 9:e1–e7. <https://doi.org/10.3832/ifer1410-007>
27. Vítková M, Tonika J, Müllerová J (2015) Black locust—successful invader of a wide range of soil conditions. *Sci Total Environ* 505:315–328. <https://doi.org/10.1016/j.scitotenv.2014.09.104>
28. Qiu L, Zhang X, Cheng J, Yin X (2010) Effects of black locust (*Robinia pseudoacacia*) on soil properties in the loessial gully region of the Loess Plateau, China. *Plant Soil* 332(1):207–217. <https://doi.org/10.1007/s11104-010-0286-5>
29. Wang MC, Wang JX, Shi QH, Zhang JS (2007) Photosynthesis and water use efficiency of *Platycladus orientalis* and *Robinia pseudoacacia* saplings under steady soil water stress during different stages of their annual growth period. *J Integr Plant Biol* 49(10):1470–1477. <https://doi.org/10.1111/j.1672-9072.2007.00561.x>
30. Bao SD (2000) Soil and agricultural chemistry analysis. Agriculture Publication, Beijing
31. Magoč T, Salzberg SL (2011) FLASH: fast length adjustment of short reads to improve genome assemblies. *Bioinformatics* 27(21):2957–2963. <https://doi.org/10.1093/bioinformatics/btr507>
32. Edgar RC (2013) UPARSE: highly accurate OTU sequences from microbial amplicon reads. *Nat Methods* 10(10):996–998. <https://doi.org/10.1038/nmeth.2604>
33. Caporaso JG, Lauber CL, Walters WA, Berg-Lyons D, Lozupone CA, Tumbaugh PJ, Fierer N, Knight R (2011) Global patterns of 16S rRNA diversity at a depth of millions of sequences per sample. *PNAS* 108 Suppl 1(Suppl 1):4516–4522. <https://doi.org/10.1073/pnas.100080107>
34. Khor WC, Roume H, Coma M, Vervaeren H, Rabaey K (2016) Acetate accumulation enhances mixed culture fermentation of biomass to lactic acid. *Appl Microbiol Biotechnol* 100(19):8337–8348. <https://doi.org/10.1007/s00253-016-7578-5>
35. Benjamini Y, Krieger A, Yekutieli D (2006) Adaptive linear step-up false discovery rate controlling procedures. *Biometrika* 93:491–507. <https://doi.org/10.1093/biomet/93.3.491>
36. Heiberger RM, Holland B (2015) Two-way analysis of variance. In: Heiberger RM, Holland B (eds) *Statistical Analysis and Data Display: An Intermediate Course with Examples in R*. Springer New York, New York, pp 377–426. [https://doi.org/10.1007/978-1-4939-2122-5\\_12](https://doi.org/10.1007/978-1-4939-2122-5_12)
37. Knights D, Kuczynski J, Charlson ES, Zaneveld J, Mozer MC, Collman RG, Bushman FD, Knight R, Kelley ST (2011) Bayesian community-wide culture-independent microbial source tracking. *Nat Methods* 8(9):761–763. <https://doi.org/10.1038/nmeth.1650>
38. Principal component analysis and redundancy analysis (2007). In: Zuur AF, Ieno EN, Smith GM (eds) *Analysing Ecological Data*. Springer New York, New York, NY, pp 193–224. doi:[https://doi.org/10.1007/978-0-387-45972-1\\_12](https://doi.org/10.1007/978-0-387-45972-1_12)
39. Ma B, Wang H, Dsouza M, Lou J, He Y, Dai Z, Brookes PC, Xu J, Gilbert JA (2016) Geographic patterns of co-occurrence network topological features for soil microbiota at continental scale in eastern China. *ISME J* 10(8):1891–1901. <https://doi.org/10.1038/ismej.2015.261>
40. Ondov BD, Bergman NH, Phillippy AM (2011) Interactive metagenomic visualization in a Web browser. *BMC Bioinformatics* 12(1):385. <https://doi.org/10.1186/1471-2105-12-385>
41. Guimera R, Nunes Amaral LA (2005) Functional cartography of complex metabolic networks. *Nature* 433(7028):895–900. <https://doi.org/10.1038/nature03288>

42. Peng GS, Wu J (2016) Optimal network topology for structural robustness based on natural connectivity. *Physica A* 443:212–220. <https://doi.org/10.1016/j.physa.2015.09.023>
43. Elser JJ, Acharya K, Kyle M, Cotner J, Makino W, Markow T, Watts T, Hobbie S, Fagan W, Schade J, Hood J, Sterner RW (2003) Growth rate–stoichiometry couplings in diverse biota. *Ecol Lett* 6(10):936–943. <https://doi.org/10.1046/j.1461-0248.2003.00518.x>
44. Meena VS, Maurya BR, Verma JP (2014) Does a rhizospheric microorganism enhance K(+) availability in agricultural soils? *Microbiol Res* 169(5-6):337–347. <https://doi.org/10.1016/j.micres.2013.09.003>
45. Wasaki J, Sakaguchi J, Yamamura T, Ito S, Shinano T, Osaki M, Kandeler E (2018) P and N deficiency change the relative abundance and function of rhizosphere microorganisms during cluster root development of white lupin (*Lupinus albus* L.). *Soil Sci Plant Nutr* 64(6):686–696. <https://doi.org/10.1080/00380768.2018.1536847>
46. Wen ZH, Li HB, Shen Q, Tang XM, Xiong CY, Li HG, Pang JY, Ryan MG, Lambers H, Shen JB (2019) Trade-offs among root morphology, exudation and mycorrhizal symbioses for phosphorus-acquisition strategies of 16 crop species. *New Phytol* 223:882–895. <https://doi.org/10.1111/nph.15833>
47. Szoboszlay M, White-Monsant A, Moe LA (2016) The effect of root exudate 7,4'-dihydroxyflavone and naringenin on soil bacterial community structure. *PLoS One* 11(1):e0146555. <https://doi.org/10.1371/journal.pone.0146555>
48. Korenblum E, Dong Y, Szymanski J, Panda S, Jozwiak A, Massalha H, Meir S, Rogachev I, Aharoni A (2020) Rhizosphere microbiome mediates systemic root metabolite exudation by root-to-root signaling. *Proc Natl Acad Sci USA* 117(7):3874–3883. <https://doi.org/10.1073/pnas.1912130117>
49. Saleem M (2015) Ecoevolutionary processes regulating microbiome community assembly in a changing global ecosystem. In: *Microbiome Community Ecology*. SpringerBriefs in Ecology. pp 55–87. doi:[https://doi.org/10.1007/978-3-319-11665-5\\_3](https://doi.org/10.1007/978-3-319-11665-5_3)
50. Shi SJ, Nuccio E, Shi Z, He ZL, Zhou JZ, Firestone M (2016) The interconnected rhizosphere: High network complexity dominates rhizosphere assemblages. *Ecol Lett* 19:919–936. <https://doi.org/10.1111/ele.12630>
51. Måren IE, Kapfer J, Aarrestad PA, Grytnes JA, Vandvik V (2018) Changing contributions of stochastic and deterministic processes in community assembly over a successional gradient. *Ecology* 99(1): 148–157. <https://doi.org/10.1002/ecy.2052>
52. Fierer N, Bradford MA, Jackson RB (2007) Toward an ecological classification of soil bacteria. *Ecology* 88(6):1354–1364. <https://doi.org/10.1890/05-1839>